Proceedings of the International Gas Turbine Congress 2003 Tokyo
November 2-7, 2003

IGTC2003Tokyo TS-063

Pressure Loss Characteristics in Rotating Coolant Passages of Gas Turbine (Effect of Inlet Flow Angle in Intermediate Shaft)

Hisashi MATSUDA[1], Fumio OTOMO[2], Asako INOMATA[2],
Kazuhiro KITAYAMA[3] and Yoshitaka FUKUYAMA[4]

[1] Power and Industrial Systems R&D Center, TOSHIBA Corporation
2-4, Suehiro-Cho, Tsurumi-Ku, Yokohama 230-0045, JAPAN
Phone: +81-45-510-5925, FAX: +81-45-500-1973, E-mail: hisashi3.matsuda@toshiba.co.jp
[2] Power and Industrial Systems R&D Center, TOSHIBA Corporation
[3] Keihin Product Operations, TOSHIBA Corporation
[4] Japan Aerospace Exploration Agency, Institute of Space Technology and Aeronautics

ABSTRACT

Pressure loss characteristics of flow inside of gas turbine intermediate shaft have been investigated experimentally using a rotating test facility with disks having diameter of 0.5m and maximum rotational speed of 4800rpm. With controlling rotational Reynolds number and coolant flow rate (Rotation number), three types of flow passages (compressor disk with straight passages, with backward swept passages and with forward swept passages) were studied and effect of inlet flow angle on pressure loss characteristics in the intermediate shaft were examined. The experiment results indicated that, comparing to the straight passages, the backward swept passages realize a major decrease of pressure loss in the intermediate shaft. On the other hand, in the case of the forward swept passages, a rapid increase of pressure loss with decreasing the Rotation number was observed.

INTRODUCTION

The coolant passages inside of both compressor and turbine disk in the recent high-temperature gas turbine have very complex configuration. The flow passage between compressor disk and turbine disk is called as “intermediate shaft”. The coolant inside of the intermediate shaft experienced a strong rotational effect. In order to improve the thermal efficiency of the gas turbine above the present state, it is very much essential to have a clear understanding of the pressure loss mechanism in this complicated flow.

Recently, we investigated pressure loss characteristics of the flow in the intermediate shaft experimentally using a rotating test facility of which is the same size as a 15MW heavy-duty gas turbine (Matsuda et al., 2000). Employing a multi-points pressure measurement system with a rotary connector not only the wall static pressure along the passage but also the total pressure in the intermediate shaft was investigated. A specially designed Kiel-tube was used to search the flow direction directly in the intermediate shaft. A compressor disk with straight passages was used in this study. From this experimental study we observed that strong swirl flow exists inside of the central pipe portion of the intermediate shaft. Kishibe & Kaji (1995) who studied numerically the flow field inside of a rotating turbine also reported the existence of strong swirl flow with non-axis-symmetric structure.

Copyright © 2003 by GTSJ
Manuscript Received on March 20, 2003

In the present study, three types of flow passages (the compressor disk with straight passages, the compressor disk with backward swept passages and the compressor disk with forward swept passages) were studied and the effect of the curved passages (inlet flow angle) on pressure loss characteristics in the intermediate shaft were examined. For all three test cases, the same turbine disk with straight passages was used. The test were done under the condition of the rotational Reynolds number $Re_\omega=1.47\times10^6 \sim 2.43\times10^6$ with the inlet Rotation number Ror $= 0.2 \sim 1.06$. The results led to an understanding that the strength of the swirl flow controls the total pressure-loss of the intermediate shaft.

NOMENCLATURE

Cp_s pressure coefficient defined by local wall static pressure $(=(P_s-P_{s2})/(\rho_o R_0^2\omega^2/2))$
Cp_ω pressure coefficient defined by local dynamic pressure $(=(P-P_2)/(\rho_o R_0^2\omega^2/2))$
Cp^*_ω pressure coefficient defined by local dynamic pressure $(=(P^*-P^*_2)/(\rho_o R_0^2\omega^2/2))$
Cp pressure coefficient defined by local velocity $(=(\rho v^2)/(\rho_o R_0^2\omega^2/2))$
d width of inlet pass (m)
P local dynamic pressure (Pa)
P_s local wall static pressure (Pa)
P^* local dynamic pressure excluding local pumping effect $(P^* = P-\rho r^2\omega^2/2)$
r local radius (m)
r_0 inner radius of central pipe (m)
R_0 outer radius of turbine disk (m)
Re_ω rotational Reynolds number $(= R_0^2\omega/\nu)$
Ro_r Rotation number $(=\omega d/U_r)$
U local mean velocity (m/s)
U_r mean velocity of inlet flow pass (m/s)
v local velocity (m/s)

<Greek symbol>
ν mean kinematic viscosity of air through flow passage (m^2/s)
ρ local density of air (kg/m^3)
ρ_o air density of exit flow pass (kg/m^3)
θ setting angle of the Keel tube(°)
ω angular velocity of rotation (rad/s)

<Subscripts>
1 inlet section of flow passage
2 outlet section of flow passage

EXPRIMENTAL SET UP

The model intermediate shaft used in the present experiment is the same size as that of a 15MW heavy-duty gas turbine (Fig.1, Ishii et al., 1998). Cross-sectional view of our experimental model is shown in Fig.2. In this model, flow of mainstream in the gas turbine is not included and we examined the pressure loss characteristics in the region starting from the inlet slit of a compressor disk to the outlet slit of a turbine disk.

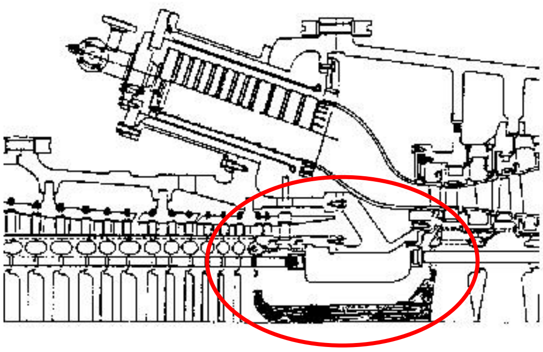

Fig.1 15MW heavy-duty gas turbine

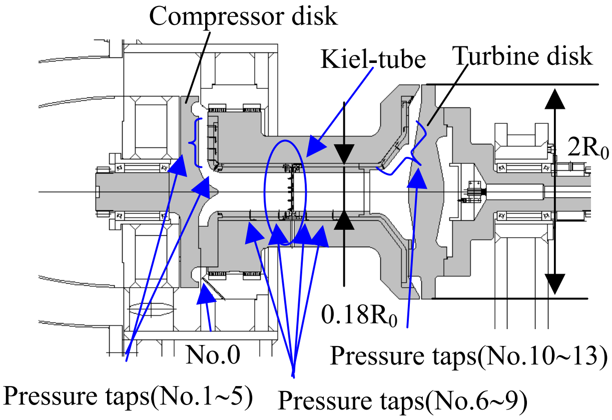

Fig.2 Cross-sectional view of the experimental apparatus

Working fluid in the present experiment was the air that supplied from a Root blower (120Nm^3/min, 8.83×10^{4}Pa). The air passed through an after-cooler section; control valves and then reached a surge tank. After the surge tank, the air passed through a pipe having inner diameter of 300mm, a flow volume meter and finally reached the test section. Inlet of the test section had a broadened outer-wall and a nose-cone type inner-wall. The air spread over smoothly between these walls and then flows into a rotational test section through an inlet-slit of the compressor disk. The central portion of the compressor disk had a total of 15 radial flow passages and the outer region of the disk comprised of a ring-shaped space. The air entered through the inlet-slit, branched through the flow passages and then converged at central pipe of the intermediate shaft. The air from the central pipe entered the turbine disk, bifurcated into a total of 12 radial flow passages and finally left the disk through an outlet-slit to a room.

In the present study, three types of flow passages were studied. The compressor disk with straight passages (Fig.3a), with backward swept passages (Fig.3b) and with forward swept passages. In the case of the forward swept passages, a reverse rotation was adapted using the disk with the backward swept passages. The value of the swept angle (23°) was determined by the limitation of a plant machine design to avoid interaction with tie-bolts. For all three test cases, the same turbine disk having straight flow passages (Fig.4) was used. The test section (from the compressor disk to the turbine disk) is rotated by an electric motor independently controlled of the Root blower.

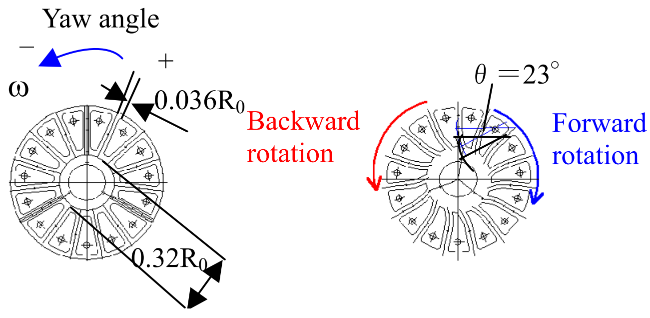

(a) Straight passages (b) Backward swept passages

Fig.3 Front view of compressor disks

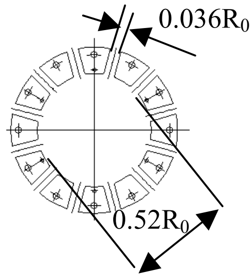

Fig.4 Front view of turbine disk

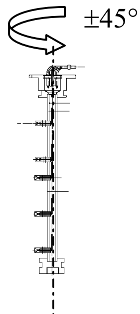

Fig.5 Kiel-tube

TEST SECTION AND MEASUREMENT TECHNIQUE

In order to examine the pressure loss characteristics of flow in the rotary test section, a total of 55-wall static pressure taps were positioned. A set of three flow passes having separated by 120 degrees from each other were selected and then a set of 5 taps were installed for each pass. At the central pipe, a total of 8 taps were installed and the rest of the taps were installed along the radial passes of the turbine. Inside of the center pipe, a Kiel-tube was also mounted to measure the total pressure in the complex flow directly. Schematic diagram of the Kiel-tube is shown in Fig.5. This Kiel-tube has a total of 5 pressure taps positioned at different radial locations and has almost flat response for a uniform flow with setting angle of –10°~+10°. The Kiel-tube was designed to be able to rotate on the axis of it own (yaw angle, interval 15°) for searching direction of the flow, but the maximum yaw angel was limited ±45° because of the interaction of the connecting tubes. Along the flow passages, thermocouples (K-type) were also installed to measure air temperature.

All the pressure-taps were connected through Teflon-tubes to a pressure-sensor package (ZOC33, SCANNING VALVE) which was mounted at the central portion of the turbine disk and rotated together with the rotary test section. By mounting sensitize-surfaces of the sensors perpendicular to the rotational axis, effect of centrifugal force was removed from the detected pressure values. By employing a brush-type slip ring (37-Poles, SOLTON), detected pressure data and temperature data were transmitted from the rotating field to the stationary field. A personal computer was used to control the pressure sensor and collect pressure and temperature data. Note that in the present experimental results, additional pressure-differences causing by the rotational effect have been corrected (Matsuda et al., 2001).

The characteristics of pressure loss were evaluated on the basis of total pressure-loss along the flow passage in the present study. However, it is hard to measure velocities in the flow passages directly under such high-speed rotating condition. Therefore, we measured the total volume flow rate by using a flow meter located at the inlet portion of the test section. From this total flow volume, local velocity at each flow passage was calculated as an area-averaging velocity by dividing a local flow volume to a local cross-section area. Each local cross-section area was defined as a flow passes-through area that perpendicular to the surface where each pressure-tap was located.

EXPERIMENTAL RESULTS

Pressure variation along the flow passages

Non-dimensionalized momentum equations in the rotational cylindrical coordinate system show that a rotational flow field like the one considered in the present study is mainly governed by two parameters namely, the rotational Reynolds number Re_ω and the Rotation number Ro_r (for example Mochizuki et al., 1992).

After performing the flow balance check, the wall static pressure variations along the flow passage of the test section were investigated for various combination of the rotational Reynolds number with the Rotation number. A typical result on pressure distribution for $Re_\omega = 2.43\times10^6$ with Ro_r =0.63 for the straight flow passages is shown in Fig.6. The uncertainty of Cp_s was ±0.047. In Fig.6, the abscissa denotes the normalized axial position. The position “0” corresponds to just after the inlet-slit of the compressor disk and the position “1” corresponds to just before the outlet-slit of the turbine disk (see also Fig.2). The variation of cross-section area of the passage, normalized by the cross-section area of the inlet-slit of the compressor disk, is also shown in Fig.6. Obviously pressure-drops were observed both in the junction region (inlet of the central pipe) and in the branching region (outlet of the central pipe).

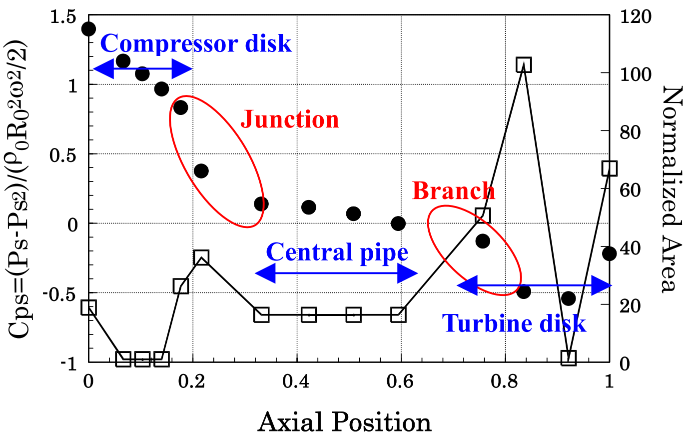

Fig.6 An example of wall static pressure variation (Re_ω=2.43×10^6 , Ro_r =0.63)

In Figs.7(a,b,c), the pressure variations with the change in the Rotation number, that means changing the inlet flow volume, but for fixed the rotational Reynolds number of $Re_\omega = 2.43\times10^6$ are shown for the straight flow passages (Fig.7a), the backward swept passages (Fig.7b) and the forward swept passages (Fig.7c). In the case of the backward swept passages (Fig.7b), the values of Cp_s decrease almost half that of the straight passages (Fig.7a) for all the Rotation number tested. And the values of Cp_s for the backward swept passages are almost the same with the decrease in the Rotation number (except for Ro_r =0.2). On the other hand, in the case of the forward swept passages (Fig.7c) the pattern of the pressure-drop and pressure-rise are similar for that of the straight passages for Ro_r >0.45, however with decrease Ro_r the values

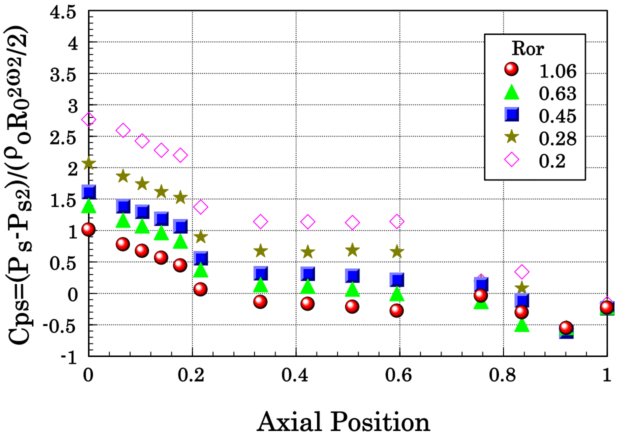

(a) Straight passages

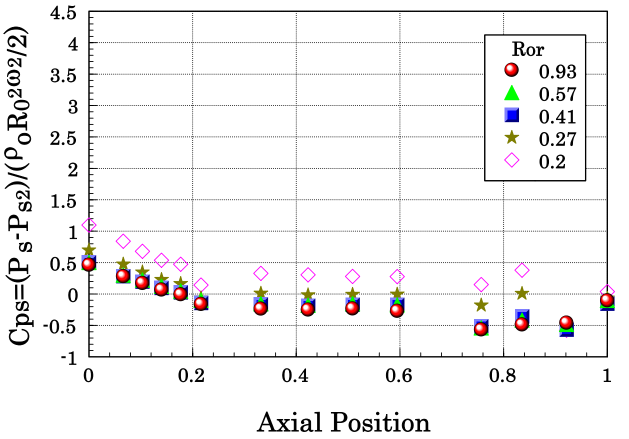

(b) Backward swept passages

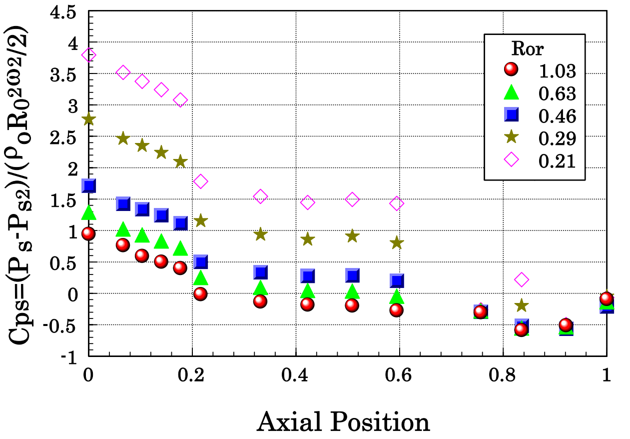

(c) Forward swept passages

Fig.7 Effect of Rotation number on wall static pressure (Re_ω=2.43×10^6)

of Cp_s for the forward swept passages increase rapidly compared to that of the straight passages.

Adding dynamic pressure to above mentioned wall static pressure, we can estimate a total pressure loss in the test section. Figs.8(a,b,c) show the total pressure variations along the flow passage for the straight passages (Fig.8a), the backward swept passages (Fig.8b) and the forward swept passages (Fig.8c). In the results presented in Figs.8(a,b,c), the ordinate represents the pressure coefficient defined on the basis of total pressures not by wall static pressures. In the present study, averaged velocity through the test section were not so high, therefore very similar type pressure variations as to Figs.7(a,b,c) are obtained.

From these figures, the variations of inlet total pressure with the Rotation number were estimated as shown in Fig.9. Adapting the backward swept passages results in a major decrease in the inlet total pressure compared to the straight passages. The degree of this pressure-loss decrease becomes remarkable with decrease in the Rotation number, the inlet total pressure of the backward swept passages at Ro_r= 0.45 (this condition corresponds to the plant condition) is about 65% of that of the straight passages. On the other hand, the inlet total pressure of the forward swept passages shows a slight decrease for Ro_r= 0.45~1.0, however, shows a rapid increase for Ro_r< 0.45 compared to the straight passages.

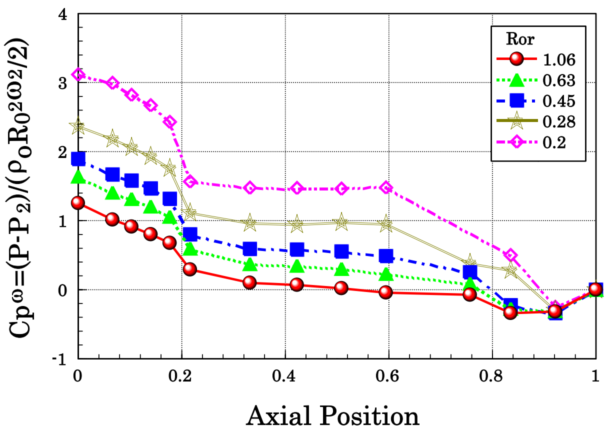

(a) Straight passages

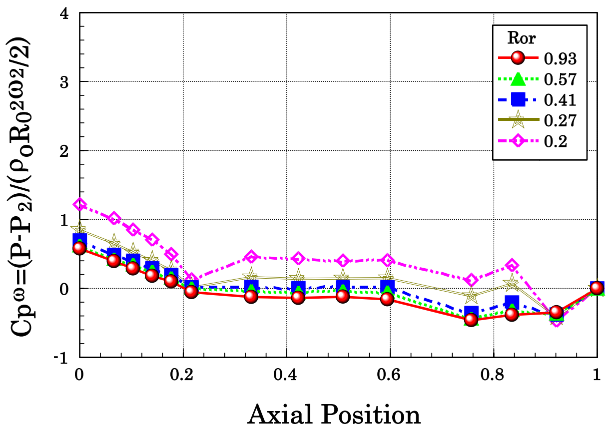

(b) Backward swept passages

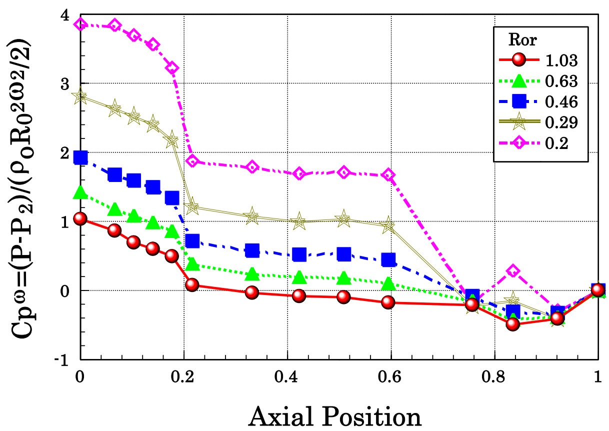

(C) Forward swept passages

Fig.8 Effect of Rotation number on total pressure (Re_ω=2.43×10^6)

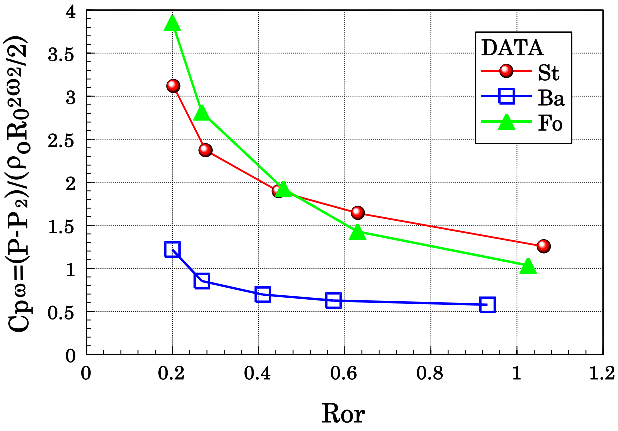

Fig.9 Variation of the inlet total pressure

Pressure distribution inside of the central pipe

The area-averaging velocity was used to estimate the dynamic pressure in the present study. In consequence, especially in the central pipe portion, there occurs some discrepancy between the estimated total pressure value on the basis of the assumption of the area-averaging velocity and the directly measured total pressure value. Therefore, we examined the flow inside of the central pipe portion by using the Kiel-tube and tried to measure the total pressure directly.

Figs.10-12(a,b,c) show the pressure distributions inside of the central pipe measured by using the Kiel-tube. In all these figures, the rotational Reynolds number is kept constant at Re_ω= 2.43×10^6 but the Rotation number is changed. Each of Fig.(a) is the result for Ro_r =1.06, Fig.(b) is that for Ro_r =0.63 and Fig.(c) is that for Ro_r =0.45, respectively. The results for the straight passages are shown in Figs.10(a,b,c), for the backward swept passages and for the forward swept passages are shown in Figs.11(a,b,c) and Figs.12(a,b,c), respectively. In these figures, the ordinate represents the total pressure coefficient and the abscissa represents normalized radius of the central pipe. The value of "r/r_0=0" means the pipe center. By adjusting the setting angle θ of the Kiel-tube, all measurements were performed. It should be noted that the results for r/r_0=0.9 in Figs.10(a,b,c) are missing because of an experimental trouble (kink of connecting-tube).

In the case of the straight passages (Figs.10a~c), where for θ= 45°, Cp_ω exhibits higher values for the entire measurement region (r/r_0=0~1). With the decrease in the setting angle, the values of Cp_ω decrease for almost the entire region. Also, Cp_ω for θ= -15°~-45° shows lower values for the entire region. These experimental facts indicate that there occurs some kind of flow deviation, namely a swirl flow, inside of the central pipe. Figs.10(a,b,c) also indicate that the swirl velocity has the maximum value around r/r_0=0.7 and decreases with decreasing r/r_0. It means that the swirl flow is biased inside of the central pipe due to the centrifugal force. Moreover, with a decrease in the Rotation number, equals to an increase in the coolant flow rate, it seems that the value of the peak of Cp_ω increases. It suggests that the biased flow is accelerated owing to put out effect of the centrifugal force, and as consequence, the swirl velocity becomes larger.

On the other hand, in the case of the backward swept passages (Figs.11a~c), where for θ= 30°~45°, Cp_ω exhibits higher values for r/r_0=0~1 and Cp_ω for θ= -30°~-45° shows lower values for r/r_0=0~1. However, the level of Cp_ω is much lower compared to the straight passages. It means the swirl flow is much weaker than that of the straight passages.

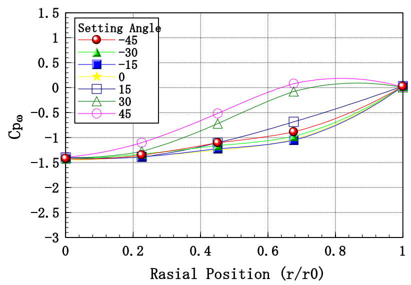

(a) Ro_r =1.06

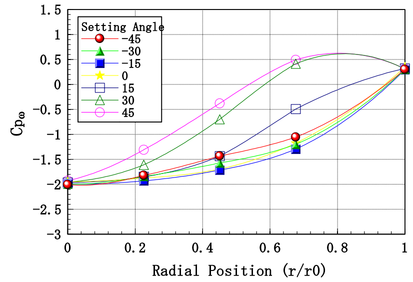

(b) Ro_r =0.63

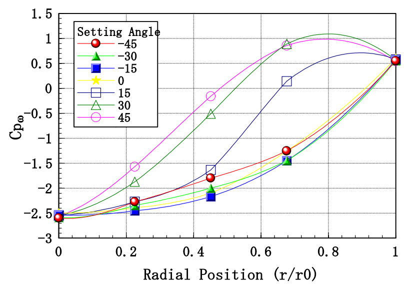

(c) Ro_r =0.45

Fig.10 Pressure distribution inside of the central pipe (Straight passages, Re_ω=2.43×10^6)

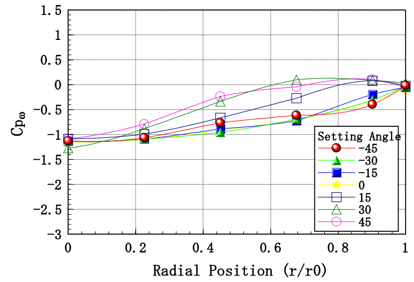

(a) Ro_r =0.93

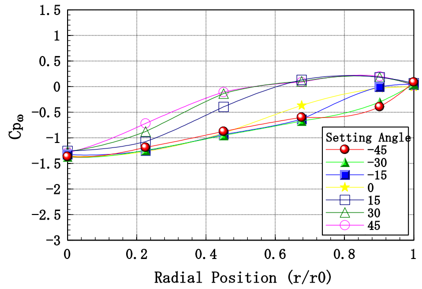

(b) Ro_r =0.57

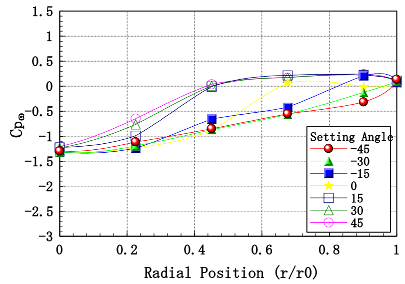

(c) Ro_r =0.41

Fig.11 Pressure distribution inside of the central pipe (Backward swept passages, Re_ω=2.43×10^6)

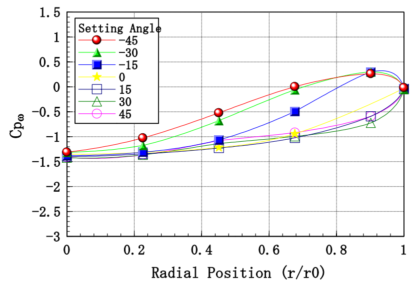

(a) Ro_r =1.03

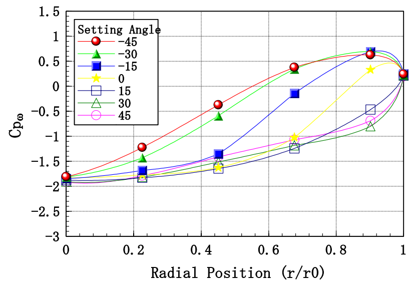

(b) Ro_r =0.63

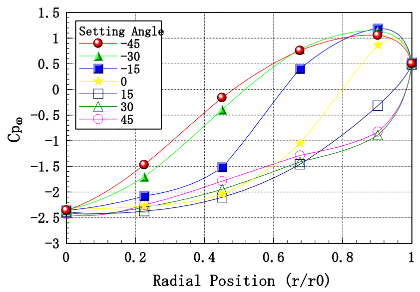

(c) Ro_r =0.46

Fig.12 Pressure distribution inside of the central pipe (Forward swept passages, Re_ω=2.43×10^6)

On the contrary, in the case of the forward swept passages (Figs.12a~c), where for θ= -45°, Cp_ω exhibits higher values for the entire measurement region (r/r_0=0~1) and where for θ= -15°~-45°, Cp_ω shows lower values for the entire region. Each peak level of Cp_ω is almost the same as that of the straight passages. These results indicate that a reverse swirl flow, the opposite rotation that for straight passages, which has almost the same swirl strength was realized in the case of the forward swept passages.

Due to the limitation of a setting angle of the Kiel-tube, we could not clarify the swirl angles exactly based on the results of these studies, and therefore, we could not obtain the exact total pressure distributions inside of the central pipe. However, judging from the tendency of the variation of Cp_ω with the setting angle of the Kiel-tube, for example in the case of the straight passages, it can be deduced that the swirl angle becomes somewhat larger than θ=45°, but the variation of Cp_ω has not changed so much. And therefore, by using these figures, it is possible to calculate an approximate swirl velocity in the following way. For the straight passages for example, firstly, suppose that the variation of Cp_ω for θ=45° as the total pressure distribution because of this variation has the largest Cp_ω value and also suppose that the variation of Cp_ω for θ=-15° as the static pressure distribution because of this variation has the least Cp_ω value. Secondly, interpolate pressure data of both θ=45° and θ=-15° with radial positions. Thirdly, find the maximum pressure difference ΔP, and then convert this maximum pressure difference to the velocity "v" using the relation as $\Delta P=\rho v^2/2$.

In a similar manner, we evaluated pressure coefficient $Cp=(\rho v^2)/(\rho_o R_0^2\omega^2/2)$ of all the swirl velocities tested as shown in Table 1. The maximum uncertainty of Cp was estimated as ±0.05. In each Ro_r number condition, almost the same Cp value is observed for both the straight passages and for the forward passages. Also the values of Cp increase rapidly with the decrease in the Ro_r number for both the straight passages and for the forward passages. On the other hand, for the backward passages, only a slight increase was observed in the value of Cp with the decrease in the Ro_r number. Therefore, with decreasing the Ro_r number, the difference between the Cp values of the straight passages and that of the backward swept passages becomes remarkable.

Table 1. Non-dimosionalized swirl velocity

	Straight	Backward	Forward
$Ro_r \cong 1.0$	Cp=1.44	0.93	1.54
$Ro_r \cong 0.6$	2.46	1.13	2.41
$Ro_r \cong 0.45$	3.19	1.21	3.25

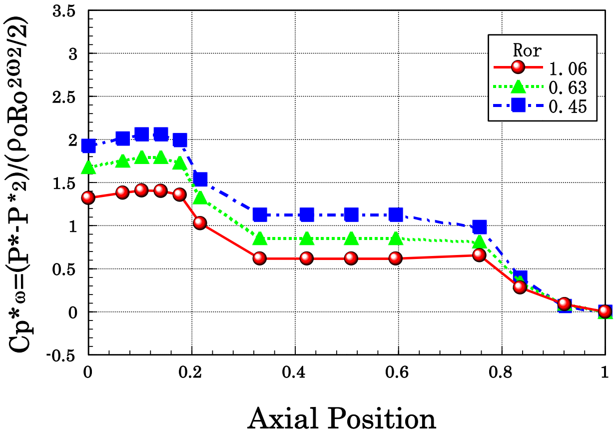

(a) Straight passages

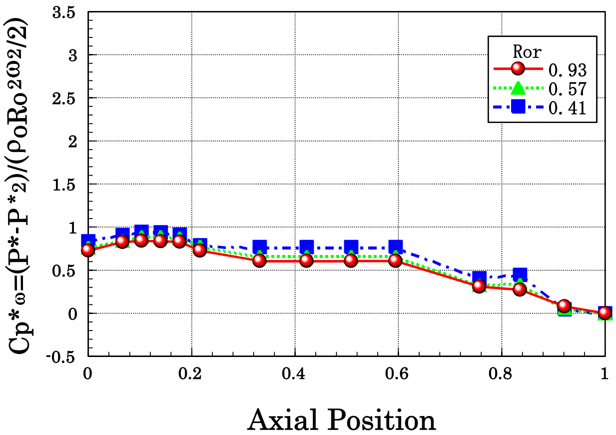

(b) Backward swept passages

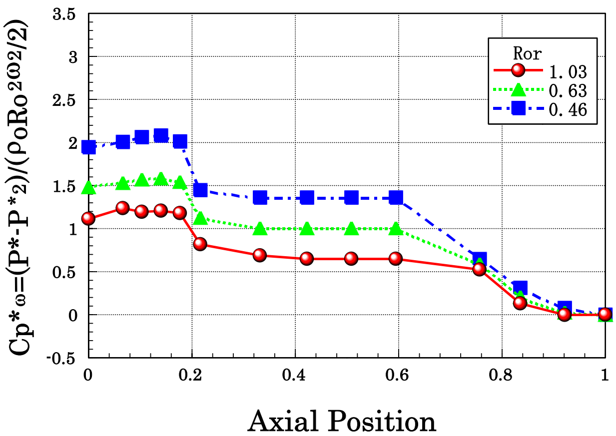

(c) Forward swept passages

Fig.13 Variation of the total pressure without pumping effect (Re_ω=2.43×10^6)

Corrected pressure variation along the flow passage

If the pumping effect ($\rho r^2\omega^2/2$) is excluded from the total pressure, the rotational effect on the characteristics of the pressure loss can be observed more clearly. In Figs.13(a,b,c), the variation of a total pressure coefficient $Cp_\omega{}^*$ defined by the pressures without including the pumping effect are shown for the straight flow passages (Fig.13a), the backward swept passages (Fig.13b) and the forward swept passages (Fig.13c), respectively. We should note that the dynamic pressures in the central pipe portion were deduced from the averaged swirl velocity. Namely, for example in the straight passages, suppose that the variation of Cp_ω for θ=45° as the total pressure distribution and the variation of Cp_ω for θ=-45° as the static pressure distribution. From this local pressure difference, the local swirl velocity can be evaluated.

Figs.13(a,b,c) indicate that there is little pressure loss both in the inlet pass and inside of the central pipe for all flow passages tested. A slight increase of $Cp_\omega{}^*$ in the inlet section (from position 0 to 0.1) for each figure implies that the flow is accelerated in the inlet slit of the compressor disk. It should be emphasized that, for entire region (including the branch region), almost flat variation of $Cp_\omega{}^*$ is realized in the case of the backward swept passages. This fact implies that control of strength of the swirl flow at the exit of the compressor disk affects not only in the junction region but also in the branching region.

From Figs.13(a,b,c), pressure differences at the junction region (from position 0.18 to 0.33) and the branching region (from position 0.59 to 0.92) are extracted then plotted in Fig.14 and Fig.15, respectively. In the junction region(Fig.14), the result for the straight passages exhibits the largest pressure difference, and that of the forward swept passages exhibits the second-largest pressure difference, while the smallest pressure difference is exhibited by the backward swept passages. We note that pressure difference is nearly the same for all the Rotation numbers tested for each type of flow passages. On the other hand, in the branching region (Fig.15), pressure differences become larger with the decrease in the Rotation number for all flow passages tested. And it should be emphasized that the forward swept passages exhibits the largest pressure difference among three passages tested. Since using the same turbine disk flow passages, configuration in the branching region is the same for all three flow passages tested. Therefore, results in Fig.15 mean the swirl flow in the junction region survives through the pipe portion and affects strongly in the branching region. And this effect becomes larger with decreasing the Rotation number.

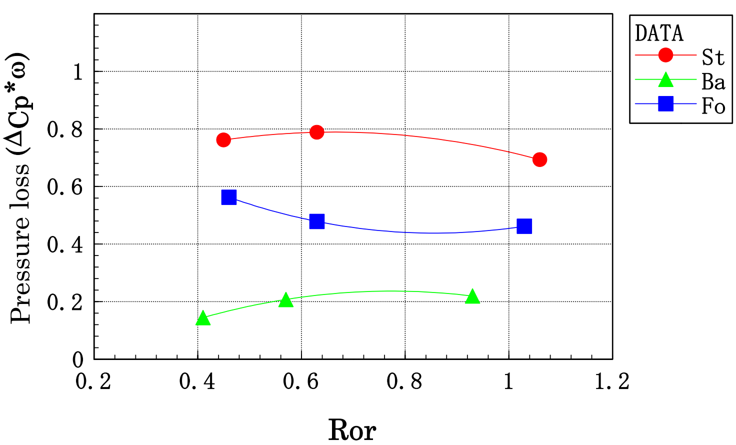

Fig.14 Pressure losses in Junction region (without pumping effect)

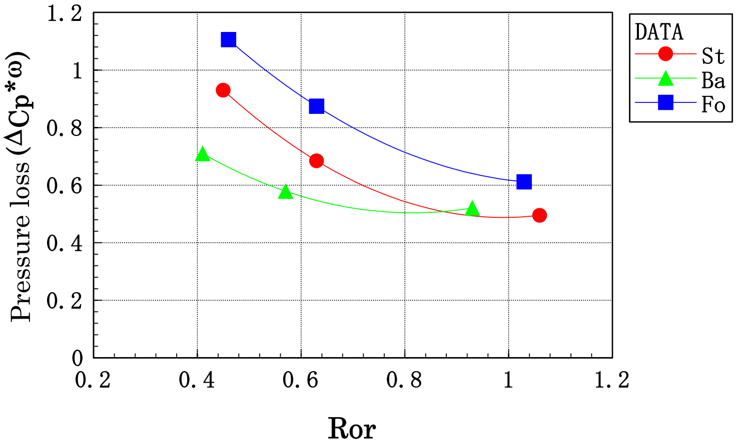

Fig.15 Pressure losses in Branching region
(without pumping effect)

CONCLUSIONS

Pressure loss characteristics of the intermediate shaft have been investigated experimentally by using a rotational test facility. With controlling the rotational Reynolds number and the Rotation number, three types of flow passages (the compressor disk with straight passages, with backward swept passages and with forward swept passages) were studied and the effect of the inlet flow angle on pressure loss characteristics in the intermediate shaft were examined. Results of the present study led to the following conclusions.

(1) Adapting the backward swept passages results in a major decrease in total pressure-loss compared to the straight passages. With decreasing the Rotational number, equals to an increase in the coolant flow rate, this decrease of pressure-loss becomes remarkable.

(2) The backward swept passages of the compressor disk leads to a major decrease of pressure-loss not only in the junction region but also in the branching region of the intermediate shaft.

(3) Compared to the straight passages, the forward swept passages leads to a slight decrease of total pressure-loss for Ro_r= 0.45~1.0, however, leads to a rapid increase for Ro_r< 0.45 in the present study.

(4) By using the forward swept passages, pressure-loss in the junction region decreases, however, pressure-loss in the branching region increases compared to the straight passages.

(5) The swirl velocity in the central pipe portion is almost the same for the straight passages and for the forward swept passages. The flow in the central pipe portion has biased configuration in radial direction and this biased flow is accelerated owing to put out effect of the centrifugal force. With the decrease in the Rotational number, equals to an increase in the coolant flow rate, the swirl velocity becomes larger for both cases.

On the other hand, the swirl flow in the backward swept passages is much weaker than that of the straight passages (or Forward swept passages). As consequence swirl velocity in the backward swept passages shows less increase with decreasing the Rotational number.

(6) The swirl flow in the junction region survives through the pipe portion and affects strongly in the branching region. And this effect becomes larger with decreasing the Rotation number

REFERENCES

(1) Matsuda, H., Otomo, F., Inomata, A., Fukuyama, Y., and Ishii, J., Pressure Loss Characteristics in Rotating Coolant Passages of Gas Turbine, (2000), JSME International Journal, Series B, Vol.43, No.4, pp.614-621.
(2) Kishibe, T. and Kaji, S., Study on the Flow Field of an Internal Cooling Air System through a Hollow Turbine Shaft, (1995), Proceedings of 1995 YKOHAMA International Gas Turbine Congress, (1995), Vol.II, pp.383-390
(3) Ishii, J., Sato, I. and Fukuyama, Y., Development and Testing of the 15MW Class Heavy Duty Gas Turbine, CIMAC Congress 1998 Copenhagen, (1998), pp.479-490.
(4) Mochizuki, S., Takamura, J., Yamawaki, S. and Yang, W., J., (1992), Heat Transfer in Serpentine Flow Passages with Rotation, ASME Paper 92-GT-190.